

Attribute-Aware Representation Rectification for Generalized Zero-Shot Learning

Zhijie Rao¹, Jingcai Guo^{1,2,*}, Xiaocheng Lu⁴, Qihua Zhou¹,
Jie Zhang¹, Kang Wei¹, Chenxin Li³, and Song Guo⁴

¹Department of Computing, The Hong Kong Polytechnic University, Hong Kong SAR

²Hong Kong Polytechnic University Shenzhen Research Institute, China

³Department of Electronic Engineering, The Chinese University of Hong Kong, Hong Kong SAR

⁴Department of CSE, Hong Kong University of Science and Technology, Hong Kong SAR

{zhijie.rao, jc-jingcai.guo, qi-hua.zhou, jie-comp.zhang, adam-kang.wei}@polyu.edu.hk

{xiaocheng.lu, songguo}@cse.ust.hk, chenxinli@link.cuhk.edu.hk

Abstract

Generalized Zero-shot Learning (GZSL) has yielded remarkable performance by designing a series of unbiased visual-semantic mappings, wherein, the precision relies heavily on the completeness of extracted visual features from both seen and unseen classes. However, as a common practice in GZSL, the pre-trained feature extractor may easily exhibit difficulty in capturing domain-specific traits of the downstream tasks/datasets to provide fine-grained discriminative features, i.e., domain bias, which hinders the overall recognition performance, especially for unseen classes. Recent studies partially address this issue by fine-tuning feature extractors, while may inevitably incur catastrophic forgetting and overfitting issues. In this paper, we propose a simple yet effective Attribute-Aware Representation Rectification framework for GZSL, dubbed (AR)², to adaptively rectify the feature extractor to learn novel features while keeping original valuable features. Specifically, our method consists of two key components, i.e., Unseen-Aware Distillation (UAD) and Attribute-Guided Learning (AGL). During training, UAD exploits the prior knowledge of attribute texts that are shared by both seen/unseen classes with attention mechanisms to detect and maintain unseen class-sensitive visual features in a targeted manner, and meanwhile, AGL aims to steer the model to focus on valuable features and suppress them to fit noisy elements in the seen classes by attribute-guided representation learning. Extensive experiments on various benchmark datasets demonstrate the effectiveness of our method¹.

*Jingcai Guo is the corresponding author.

¹The code is available at: github.com/zjrao/AARR

1. Introduction

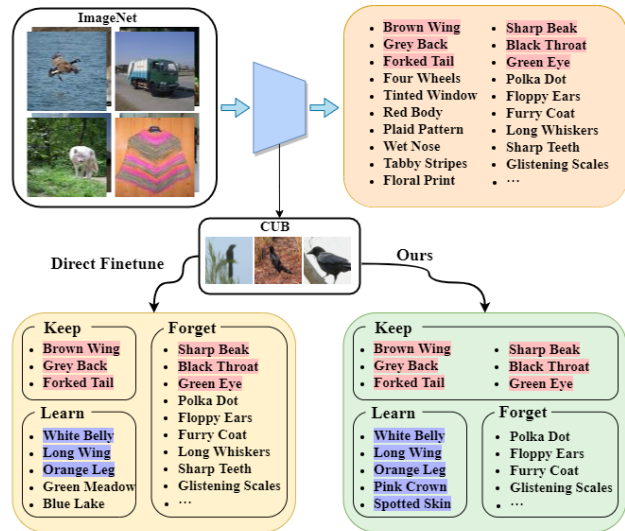


Figure 1. Pink indicates features that are beneficial to the downstream data. Purple indicates newly learned valuable features. Pre-trained models lack the ability to extract fine-grained information of specific datasets. Direct fine-tuning leads to forgetfulness and overfitting, whereas our approach aims to keep and learn valuable information (better viewed in color).

The success of deep neural networks in the visual area is well documented, and one of the reasons is the support of a huge amount of training data. Nevertheless, it is an intractable condition to fulfill in the real-world scenario, e.g., there are very few or even no samples of rare species. To solve this problem, Zero-Shot Learning (ZSL) has gained increasing attention in recent years with its ded-

ication to bridging the gap between language and vision, which takes inspiration from the logical reasoning ability of human beings. By virtue of the shared visual information and the semantic descriptions of unseen classes, ZSL endows the model with out-of-distribution recognition capability. Another more challenging task is Generalized Zero-Shot Learning (GZSL), which requires simultaneous recognition of both seen and unseen categories [2, 22].

Mainstream studies strive to search and locate local visual attributes so as to construct one-to-one visual-semantic mappings [5, 6, 13, 33, 42, 43, 46], or implicitly learn the class-wise visual-semantic relation to simulate unseen distributions in a generative manner [11, 19, 24, 35, 36, 40, 44, 47]. Despite the promising results achieved by these approaches, the visual-semantic matchiness is significantly restricted by the incompleteness of the visual features. Such deficiency stems from the domain bias between the pre-trained dataset, e.g., ImageNet [10], and the downstream tasks/datasets, which simply states that the extracted features are insufficient to provide fine-grained knowledge to build complete and reliable visual-semantic pairs [3].

To address such issues, a straightforward solution is to fine-tune them on downstream tasks, which may inevitably introduce catastrophic forgetting and overfitting problems (Fig. 1) [16, 23]. Concretely, deep neural networks usually excel at seeking shortcuts from observed data [12], favoring partial features that benefit the seen classes during the fine-tuning process, while conversely, features that are critical for the unseen classes may be filtered. Meanwhile, newly learned features may contain various noise, e.g., backgrounds, irrelevant attributes, etc., rendering the model to create pseudo-visual-semantic associations. Worse still, identical issues also exist in the realm of continual learning [9] and spawn substantial mature schemes. However, they are not applicable to ZSL/GZSL, which has no further training or adjustment phase for novel categories.

Grounded on the above discussions, we lock our research interests in the following two aspects: 1) *How to keep the valuable knowledge in the raw features to ensure the unseen distributional generalizability of the model*, and 2) *How to guide the learning process of new knowledge to reduce the interference of noisy factors*. The crux of these issues is to determine which features are worth being kept and learned. In this paper, we argue that attributes, i.e., textual descriptions or semantic embeddings, are the only shared supervisory signals to distinguish seen and unseen classes. Thus, the kept and learned features need to be directed by them.

Hereby, we present the **A**tttribute-**A**ware **R**epresentation **R**ectification framework for GZSL, i.e., $(AR)^2$, to adaptively rectify the feature extractor to learn novel features while keeping original valuable features. Concretely, our $(AR)^2$ consists of two key components including Unseen-Aware Distillation (UAD) and Attribute-Guided Learning

(AGL). The objective of UAD is to identify those in the raw features that are beneficial to both seen and unseen classes. By virtue of the attention mechanism of the class activation map [34] and the attribute-region classifier [6, 17], specific features are identified and localized. Specifically, on the one hand, we use the pre-trained network as the teacher model and attribute labels of similar classes as supervisory information to obtain class activation maps of unseen classes by gradient propagation. Meanwhile, the score of the attribute-region classifier is utilized to restrict the scope of attention maps, from which valuable features are filtered out. In parallel, the student model is prompted to retain this fraction of features by means of feature distillation. On the other hand, AGL aims to encourage the model to refine features that are most relevant to attributes and reduce noisy interference. We first leverage features extracted by the teacher model to initialize visual prototypes of each sub-attribute, which form an attribute pool. Class prototypes can then be obtained by selecting and assembling various sub-attributes from the pool. The attribute pool is updated by each batch of data during the training period, with increasing the semantic distance between prototypes of each category as the learning goal. In this way, the model is implicitly motivated to learn features that are associated with attributes and are discriminative. Finally, the teacher model is updated by the exponential moving average method with the student model.

Our contributions are summarized as follows:

- To alleviate the issue of mismatch between the pre-trained model and downstream data/tasks, we present a novel method named $(AR)^2$ to adaptively rectify the feature representations. $(AR)^2$ steers the learning process with the supervision of attributes, continuously keeping and learning the most valuable knowledge.
- $(AR)^2$ consists of two main components, wherein, UAD assists the model in reviewing old knowledge to prevent catastrophic forgetting and AGL guides the model in refining features to avoid overfitting on noisy information.
- We conduct extensive experiments and analysis on three benchmark datasets, and the results show that the proposed method is effective to improve the performance of the model.

2. Related Work

2.1. Bridge Vision and Attribute

ZSL/GZSL aims to learn shared attributes (semantics) from accessible training data, thereby obtaining the ability to infer on the unknown domain [2, 22]. Attribute descriptions, i.e., text embeddings, category prototypes, etc., are the only prior information to access unseen categories. Therefore, how to connect the visual features of the seen classes with the attributes is a central issue in ZSL/GZSL. Numerous studies choose the most direct way, i.e., mapping

visual features to the attribute space [32]. In this direction, the accuracy of the mapping is the main challenge to attack. Existing approaches include generating hallucinatory categories [1], reconstructing visual features [20], and modeling region-attribute relationships [5, 13, 17, 26, 27, 38, 42, 43, 45, 46], to name a few. In contrast, some studies opt to map attributes to the visual space and adjust the mapping function by maintaining semantic relations among categories [48]. In addition to this, some studies combine the characteristics of the above two methods by mapping visual features and attributes to a common space [6, 18, 28, 33], thus mitigating the discrepancies between different modal data. Compared to modeling the visual-attribute relationship explicitly, generative approaches [11, 19, 24, 35, 36, 40, 44, 47] provide an alternative perspective, i.e., learning the relationship implicitly by means of the distributional alignment capability of GANs or VAEs. Although these approaches achieve promising results, they are limited by the domain bias problem between the pre-trained model and the downstream dataset, i.e., the pre-trained model struggles to capture the fine-grained features of the specific dataset, which is detrimental to the establishment of accurate visual-attribute associations.

2.2. Domain Bias

A common practice in ZSL/GZSL is to utilize the ImageNet [10] pre-trained model to extract features and then develop links between visual features and attributes. However, inherent domain differences exist between datasets, i.e., domain bias. For instance, ImageNet [10] lacks fine-grained annotations for birds, which are needed to discriminate samples in the CUB dataset [37]. Xian *et al.* [41] achieve performance improvement by fine-tuning the feature extractor, demonstrating the existence of domain bias. However, they do not conduct further research to mitigate the forgetting and overfitting problems [16, 23].

2.3. Representation Rectification

Domain bias leads to features extracted by the pre-trained model on the downstream dataset being incomplete, i.e., lacking fine-grained, targeted information. To this end, some studies attempt to rectify the extracted features (raw features). Li *et al.* [25] and Chen *et al.* [7] argue that the raw features contain both class-relevant and class-irrelevant parts, which are then stripped away by means of disentanglement. Chen *et al.* [3] strive to refine the raw features in order to reduce the redundancy of the information and to enhance the discriminability of the features. Han *et al.* [14], on the other hand, utilize contrastive learning to bring the same-class representations closer and push the dissimilarity of representations farther away. Kong *et al.* [21] then resort to enhancing the intra-class compactness. Although their methods mitigate the domain bias to some extent, they are

unable to learn new knowledge on downstream datasets.

3. Method

Preliminary. In the ZSL/GZSL tasks, generally, the training data consists of complete samples of seen classes and attribute vectors of unseen classes. Suppose $D^s = \{x^s, y^s, a^s\}$ denotes the seen class sample set, where x^s, y^s and a^s denote the images, labels and attributes, respectively. Let $D^u = \{a^u\}$ denote attributes of unseen classes, and $a = a^s \cup a^u$ is the whole attribute set. Meanwhile, we also use the semantic embeddings of each sub-attribute learned by GloVe, which are indicated by $v = \{v_1, v_2, \dots, v_n\}$, where n is the number of sub-attributes. Let K denote the number of categories, including seen and unseen categories. Our approach consists of a teacher model $\mathcal{T} = \{\mathcal{E}^t, \mathcal{W}^t\}$ and a student model $\mathcal{S} = \{\mathcal{E}^s, \mathcal{W}^s\}$ that have the same network structure, where $\mathcal{W}^t = [\mathcal{W}_1^t, \mathcal{W}_2^t]$ and $\mathcal{W}^s = [\mathcal{W}_1^s, \mathcal{W}_2^s]$. Each model includes a feature extractor \mathcal{E} and a classifier $\mathcal{W} = [\mathcal{W}_1, \mathcal{W}_2]$. Let w_1, w_2 denote the learnable parameters of $\mathcal{W}_1, \mathcal{W}_2$, respectively. Then w_1^t, w_2^t stand for the teacher model’s parameters, and w_1^s, w_2^s represent the student model’s. AGL module has a classifier \mathcal{W}^p , where w^p denotes the parameters.

Overview. Our approach is depicted in Fig. 2. The teacher model is responsible for retaining historical features to prevent the student model from forgetting old knowledge. UAD employs a dual filtering mechanism, i.e., class activation map and attribute scoring, to identify and locate the valuable parts of the features extracted by the teacher model. The output of UAD is a weight map, which measures the value of each region. After that, the teacher’s knowledge is passed on to the students via distillation. AGL utilizes the original and learnable features to maintain a pool of attributes that contain prototypes of each sub-attribute. Different class prototypes are available by selecting and assembling various sub-attributes. By maximizing the distance between the prototypes of each class, AGL implicitly facilitates the correlation between learned features and attributes.

3.1. Attribute-Region Classifier

Attributes are the only shared prior information between seen and unseen classes, which are crucial for identifying unknown classes. However, attribute descriptions are typically coarse-grained class-wise annotations, hence many studies resort to learning fine-grained attribute-region mapping relations. Recent works [6, 17] have achieved promising results by incorporating attention mechanisms into classifiers. Since our approach requires localizing attribute-related features (regions), we employ the same classifier.

Assume $f = \mathcal{E}(x), f \in \mathbb{R}^{CHW}$ denotes the feature of an input image extracted by the feature extractor \mathcal{E} , where C, H, W denote the channel, height, and width. Then f is

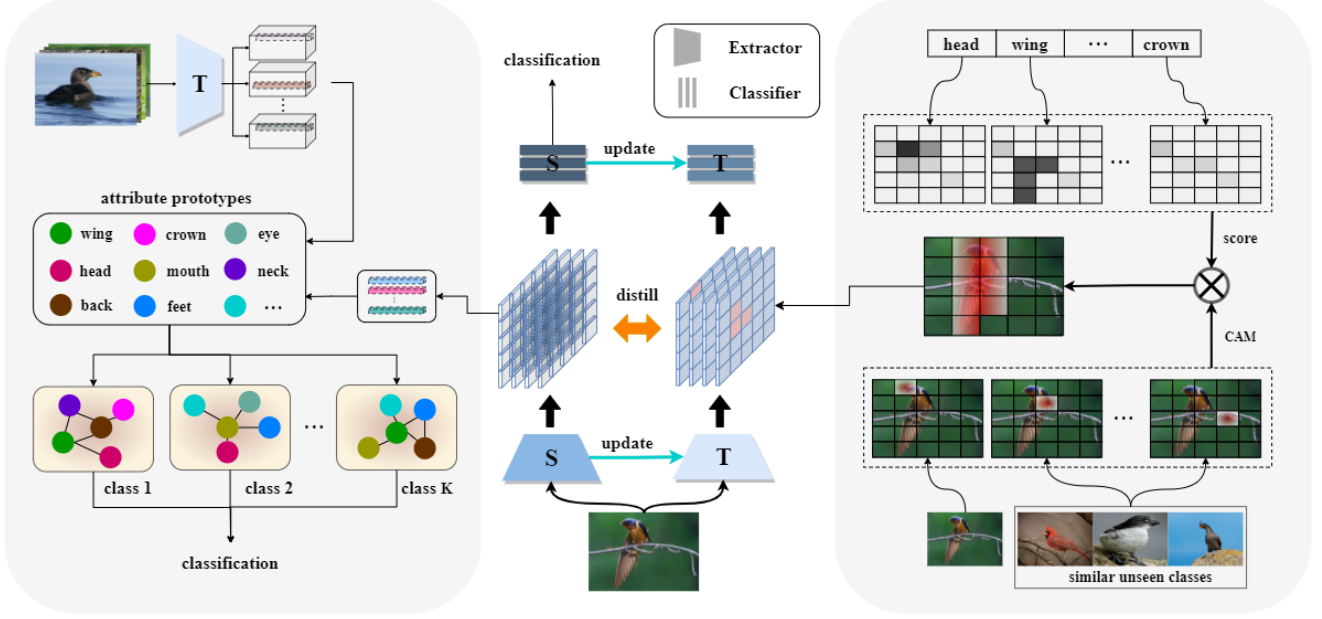


Figure 2. The overall framework of our method. ‘S’ denotes the student model and ‘T’ denotes the teacher model. UAD identifies and localizes the features extracted by the teacher model to filter the valuable parts. AGL utilizes the features extracted by the student model to update the attribute pool to facilitate the associations between the learned features and attributes (better viewed in color).

divided into $r = HW$ regions, and each region is represented by a C -dimensional vector. The degree of association between each attribute and each region can be scored, which is formulated as:

$$p(i, j|w_1) = \frac{\exp(v_i w_1 f_j)}{\sum_{q=1}^r \exp(v_i w_1 f_q)}, \quad (1)$$

where $p(i, j)$ denotes the association score of attribute i and region j . Then p is used to weight the final output and optimize it with cross-entropy loss. The loss function is defined as:

$$\mathcal{L}_{CE}(a, f, p|w_2) = -\log \frac{\exp(a(v w_2 f)p)}{\sum_{k=1}^K \exp(a_k(v w_2 f)p)}, \quad (2)$$

3.2. Unseen-Aware Distillation

Models gradually forget some important features as they learn downstream data. In order to help the model memorize these features, we design the UAD module to review the old valuable knowledge. A key issue is how to recognize which features are worth being retained. We are inspired by the class activation map [34], which indicates the correlation between regional features and classes via gradient responses. So we use the class activation maps created by the teacher model to represent the importance of each region. Let $f_t = \mathcal{E}^t(x)$ denote the feature extracted by the teacher extractor, and $o_t = \mathcal{W}^t(f_t)$ denotes the output of the teacher classifier. Then, if we want to know which regional features are strongly correlated with category c , we

just need to activate the gradient for the corresponding category and the gradient map is represented as:

$$g(k) = \tau\left(\frac{\partial \mathcal{L}_{CE}(a_c, f_t, p_t|w_2^t)}{\partial f_t}\right), \quad (3)$$

where a_c is the attribute of class c and $p_t(i, j) = p(i, j|w_1^t)$ and $\tau(\cdot)$ is Min-Max Normalization.

Unseen-Aware Attention. A simple idea is to activate the category corresponding to the training sample to get the activation map. However, such an approach would be inclined to focus on attributes that favor the seen classes, leading to overfitting, which is not conducive to generalization to the unseen classes. Therefore, we need to know which attributes the unseen classes are interested in. In the end, we activate similar unseen classes at the same time. Specifically, we first compute the similarity between the attributes of the unseen and seen classes, which is measured by Euclidean distance. Then we select the m most similar seen classes for each unseen class, corresponding to the fact that there will exist an unseen class similarity set U_k for each seen class k . After that, we get the new activation map:

$$g = \tau(g(k) + \frac{1}{d} \sum_{k_u \in U_k} g(k_u)), \quad (4)$$

where d denotes the size of set U_k .

Attribute-Aware Attention. Despite the fact that the class activation map implies connections between regions and classes, those regions may be the ones that contain noise,

such as backgrounds. For example, if the unseen class possesses the attribute *crow* while the corresponding seen class does not, then the activated region is inaccurate. To suppress the effect of this part of the regions, we reweight the activation map with the score of the attribute-region classifier. Assuming \hat{p} denotes the score map of the training sample computed by Eq. 1, the final attention map is defined as:

$$g = g \cdot \hat{p}, \quad (5)$$

where (\cdot) denotes the dot product.

Knowledge Distillation. We use feature distillation to transfer knowledge to the student model. Suppose $f_s = \mathcal{E}^s(x)$ denotes the feature extracted by the student extractor. The distillation loss is:

$$\mathcal{L}_{UAD} = \|f_s - f_t\|^2 \cdot g, \quad (6)$$

where $\|\cdot\|$ means Mean-Square Error loss function.

3.3. Attribute-Guided Learning

Another problem with the application of the model to downstream tasks is overfitting. Due to the characteristic of neural networks that are skilled at finding shortcuts [12], some noisy features, irrelevant attributes, etc. in the seen classes receive more attention, which prevents the model from generalizing to the unseen classes. The goal of AGL is to guide the model to learn features that are relevant to attributes. Our motivation is to reorganize learned features into class prototypes guided by attributes, and then implicitly enhance the connection between learned features and attributes by increasing the distinguishability of class prototypes.

Initialize Attribute Pool. We firstly create an attribute pool $h = \{h_1, h_2, \dots, h_n\}$, $h_i \in \mathbb{R}^C$, where n is the number of sub-attribute and h_i denotes the prototypical feature of the i -th sub-attribute. The attribute pool is initialized by the features extracted by the teacher model. Specifically, we compute the prototypes using the region in each sample that has the highest correlation with the attribute. According to Eq. 1, we can obtain the association score map of attributes and regions. Then the prototype of attribute i is formulated as:

$$h_i = \frac{\sum_{j=1}^N \bar{p}_i^j \bar{f}_i^j}{\sum_{j=1}^N \bar{p}_i^j}, \quad (7)$$

where \bar{p}_i^j denotes the max score of attribute i in sample j and \bar{f}_i^j is the corresponding region feature of \bar{p}_i^j . N is the size of the whole training dataset. Note that the initialization is performed only once during the entire training process, and we set h learnable.

Update Attribute Pool. During the training phase, we update the attribute pool with the features extracted from the student model. For a batch of features f_s extracted by the

student extractor, the prototype of attribute i is:

$$\bar{h}_i = \frac{1}{B} \sum_{b=1}^B \sum_{j=1}^r \frac{p^b(i, j) f_j^b}{p^b(i, j)}, \quad (8)$$

where \bar{h}_i denotes the prototype of attribute i computed by current batch and B denotes the batch size. Here $p(i, j) = p(i, j|w_1^s)$. Then the attribute pool is updated by:

$$h = h \times \lambda + \bar{h} \times (1.0 - \lambda), \quad (9)$$

where λ is a balanced parameter and we set it learnable.

Optimization Objective. We hope that the updated attribute pool can facilitate the recognition of both seen and unseen classes. Specifically, with the help of attribute vectors, class prototypes are obtained by adaptively selecting and assembling sub-attributes. Then we increase the semantic distance between the class prototypes to enhance the correlation between the learned features and attributes. The loss function is:

$$\mathcal{L}_{AGL} = -\log \frac{\exp(ahw_p)}{\sum_{k=1}^K \exp(a_k h w_p)}. \quad (10)$$

3.4. Overall Objective

In the pre-training stage, only \mathcal{L}_{CE} is used for training because the performance of the attribute-region classifier is too weak to localize valuable features. When the model is stabilized, all loss functions are used to train together. The optimization objective is:

$$\mathcal{L}_{AR} = \mathcal{L}_{CE} + \beta \mathcal{L}_{UAD} + \gamma \mathcal{L}_{AGL}, \quad (11)$$

where β and γ are hyper-parameters. The teacher model does not participate in training. At the end of each epoch, an update is performed by the exponential moving average method. Let Θ^t and Θ^s denote the parameters of the teacher model and the student model. The teacher model is updated by:

$$\Theta^t = \Theta^t \times \delta + \Theta^s \times (1.0 - \delta), \quad (12)$$

where δ is a constant and is set to 0.9995.

4. Experiments

Datasets. We perform experiments on three benchmark datasets including CUB (Caltech UCSD Birds 200) [37], SUN (SUN Attribute) [31], and AWA2 (Animals with Attributes 2) [39]. We split the seen and unseen classes according to the criteria described in [39]. CUB is a fine-grained bird dataset containing 11,788 images with 150 seen classes and 50 unseen classes, and the attribute dimension is 312. SUN is a scene dataset containing 14,340 images with 645 seen classes and 72 unseen classes, and the

Table 1. The experimental results(%) of CUB, SUN, and AWA2 on **ZSL** and **GZSL** settings. Method types are listed in the *BRANCH* column. GEN: Generative Method; OWM: One-Way Mapping; CS: Common Space; DA: Data Augmentation; and RR: Representation Rectification. The best, second-best, and third-best results are highlighted in **red**, **blue**, and underlined, respectively.

METHOD	BRANCH	CUB				SUN				AWA2			
		T	U	S	H	T	U	S	H	T	U	S	H
f-CLSWGAN (CVPR '18) [40]	GEN	57.3	43.7	57.7	49.7	60.8	42.6	36.6	39.4	68.2	57.9	61.4	59.6
f-VAEGAN-D2 (CVPR '19) [41]	GEN	61.0	48.4	60.1	53.6	64.7	45.1	38.0	41.3	71.1	57.6	70.6	63.5
TF-VAEGAN (ECCV '20) [30]	GEN	64.9	52.8	64.7	58.1	66.0	45.6	40.7	43.0	72.2	59.8	75.1	66.6
E-PGN (CVPR '20) [47]	GEN	72.4	52.0	61.1	56.2	-	-	-	-	73.4	52.6	83.5	64.6
SGMA (NeurIPS '19) [49]	OWM	71.0	36.7	71.3	48.5	-	-	-	-	68.8	37.6	87.1	52.5
AREN (CVPR '19) [42]	OWM	71.8	38.9	78.7	52.1	60.6	19.0	38.8	25.5	67.9	15.6	92.9	26.7
LFGAA (ICCV '19) [29]	OWM	67.6	36.2	80.9	50.0	61.5	18.5	40.0	25.3	68.1	27.0	93.4	41.9
DAZLE (CVPR '20) [17]	OWM	66.0	56.7	59.6	58.1	59.4	52.3	24.3	33.2	67.9	60.3	75.7	67.1
APN (NeurIPS '20) [45]	OWM	72.0	65.3	69.3	67.2	61.6	41.9	34.0	37.6	68.4	57.1	72.4	63.9
VS-Boost (IJCAI '23) [26]	OWM	79.8	68.0	68.7	<u>68.4</u>	62.4	49.2	37.4	42.5	-	-	-	-
DCN (NeurIPS '18) [28]	CS	56.2	28.4	60.7	38.7	61.8	25.5	37.0	30.2	65.2	25.5	84.2	39.1
CADA-VAE (CVPR '19) [33]	CS	59.8	51.6	53.5	52.4	61.7	47.2	35.7	40.6	63.0	55.8	75.0	63.9
HSVA (NeurIPS '21) [4]	CS	62.8	52.7	58.3	55.3	63.8	48.6	<u>39.0</u>	43.3	-	59.3	76.6	66.8
MSDN (CVPR '22) [6]	CS	76.1	<u>68.7</u>	67.5	68.1	<u>65.8</u>	52.2	34.2	41.3	70.1	<u>62.0</u>	74.5	67.7
HAS (MM '23) [8]	DA	76.5	69.6	<u>74.1</u>	71.8	63.2	42.8	38.9	40.8	71.4	63.1	<u>87.3</u>	73.3
FREE (ICCV '21) [3]	RR	-	55.7	59.9	57.7	-	47.4	37.2	41.7	-	60.4	75.4	67.1
SDGZSL (ICCV '21) [7]	RR	75.5	59.9	66.4	63.0	62.4	48.2	36.1	41.3	<u>72.1</u>	64.6	73.6	68.8
CE-GZSL (CVPR '21) [14]	RR	<u>77.5</u>	63.9	66.8	65.3	63.3	48.8	38.6	<u>43.1</u>	70.4	63.1	78.6	70.0
(AR)²(Ours)	RR	80.2	74.1	73.0	73.5	66.2	<u>51.9</u>	37.8	43.7	70.9	61.5	81.2	70.0

Table 2. The results(%) of ablation study. ‘*’ denotes MSDN [6] as the baseline. ‘✓’ denotes adding the module. The best results are marked in **bold**.

METHOD	UAD	AGL	CUB		SUN		AWA2	
			T	H	T	H	T	H
Baseline*			76.1	68.1	65.8	41.3	70.1	67.7
Finetune			78.5	71.8	63.8	42.0	68.4	67.3
Ours-1	✓		79.7	73.0	65.4	42.9	69.5	68.4
Ours-2		✓	79.1	72.2	64.5	42.1	68.3	67.5
Ours	✓	✓	80.2	73.5	66.2	43.7	70.9	70.0

attribute dimension is 102. AWA2 is a coarse-grained animal dataset containing 37,322 images, including 40 seen classes and 10 unseen classes, and the attribute dimension is 85.

Evaluation Protocols. For the **ZSL setting**, we evaluate the top-1 accuracy on unseen classes and denote it as **T**. For the **GZSL setting**, we record the top-1 accuracies on seen and unseen classes and denote them as **S** and **U**, respectively. Meanwhile, we report their harmonic mean **H**, i.e., $H = \frac{2SU}{S+U}$, to evaluate the performance of GZSL.

Implementation Details. We adopt the feature extractor of ResNet101 [15] pre-trained on ImageNet [10] and the classifier of MSDN [6] to form our network architecture. The batch size is set to 32 for CUB and 50 for SUN and AWA2. We set the learning rate to 5e-6 and employ the RMSProp optimizer with the momentum set as 0.9 and weight decay

set as 1e-4. For hyperparameters, we set m to 5 for AWA2 and 10 for CUB and SUN. For β and γ , we set them to $\{10, 0.1\}$ for CUB and AWA2 and $\{15, 0.1\}$ for SUN.

4.1. Comparison with State-of-the-Arts

We compare our $(AR)^2$ with state-of-the-art methods of various types, including GEN (Generative Method), OWM (One-Way Mapping, i.e., visual feature maps to attribute space or attribute maps to feature space), CS (Common Space), RR (Representation Rectification). The experimental results are shown in Table 1. As can be seen from the table, our method yields competitive results, with the highest H-scores and ZSL accuracies on both the CUB and SUN datasets. Specifically, our H-score on CUB precedes the second place by 1.7%, and the recognition rate of unseen classes (74.1%) precedes the second place by 4.5%. On the SUN dataset, we achieve an H-score of 43.7% and a T-score of 66.2% for the first and third places, respectively. Five of our metrics achieve the best scores, one second and one third. Notably, our scheme is also far ahead of its peers. The experimental results show that the features extracted from the pre-trained model have great room for improvement and that representation rectification is one of the effective schemes. Meanwhile, our solution significantly contributes to the recognition performance with dual constraints of keeping and learning valuable knowledge.

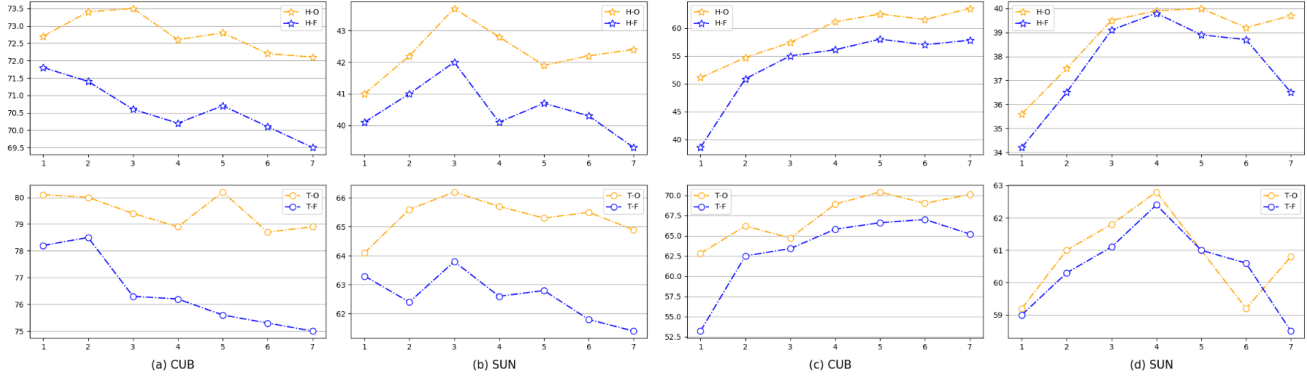


Figure 3. Comparison of the stability of our method with finetune. *H-O*: H score of our method. *H-F*: H score of Finetune. *T-O*: T score of our method. *T-F*: T score of Finetune (better viewed in color).

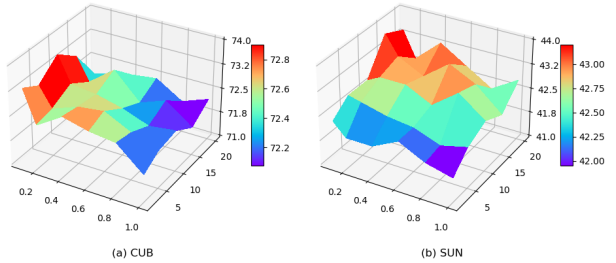


Figure 4. The analysis of sensitivity to hyperparameters β and γ (better viewed in color).

4.2. Ablation Study

We perform a series of ablation experiments to analyze the functionality of each component. We use MSDN as the baseline and compare our method with direct fine-tuning. The results of the experiments are shown in Table 2, where it can be seen that fine-tuning brings some boost on the CUB and SUN datasets, but does not significantly promote the effect on AWA2. Our method, instead, achieves the best results on all three datasets, and each component plays a positive role. It demonstrates the soundness of the design of each component and the effectiveness of our method in mitigating the forgetting and overfitting problems.

4.3. Analysis of Hyperparameters

Sensitivity of β and γ . We conduct a number of experiments to analyze the sensitivity of the hyperparameters β and γ . The experimental results are shown in Fig. 4. We set β to [1, 5, 10, 15, 20] and γ to [0.1, 0.2, 0.4, 0.6, 0.8, 1.0], respectively. Fig. 4 (a) and (b) show the performance plots of the H-score on CUB and SUN, respectively. As can be seen from the figure, changes in β and γ do not lead to large fluctuations in performance. And, we recommend setting β to [10, 15] and γ below 0.5 for optimal performance.

Effect of m and λ . We further analyze the impact of the parameter m , i.e., how many of the most similar seen classes are appropriate to choose among the UDA module. The experimental results are shown in Table 3. We set m to [1, 5, 10] for comparison, and the experimental results on CUB show that setting it to 10 is best, but setting it to 5 is better on AWA2. The reason is that CUB has a total of 200 classes with 150 seen classes, while AWA2 has a total of only 50 classes with 40 seen classes. Moreover, AWA2 is a coarse-grained dataset with less similarity between categories. In addition, we investigate the effect of the parameter λ in Eq. 9. The experimental results are also shown in Table 3. We conduct experiments on the CUB and SUN datasets by fixing it to [0.9, 0.5]. The results show that the fixed values are not as effective as the learnable ones.

Table 3. The effect of the number m of similar seen classes and the parameter λ in Eq. (9).

SETTING	CUB		AWA2	
	T	H	T	H
$m = 1$	79.6	72.1	69.6	69.0
$m = 5$	79.5	73.0	70.9	70.0
$m = 10$	80.2	73.5	69.1	68.7
SETTING	CUB		SUN	
	T	H	T	H
$\lambda = 0.9$	78.4	72.5	64.9	43.0
$\lambda = 0.5$	79.6	72.9	64.5	42.8
$\lambda = \text{learnable}$	80.2	73.5	66.2	43.7

4.4. Stability Analysis

We conduct a plethora of experiments to analyze the stability of our method and compare it with fine-tuning. We study the effect of training time as well as learning rate on performance to analyze the contribution of our method in

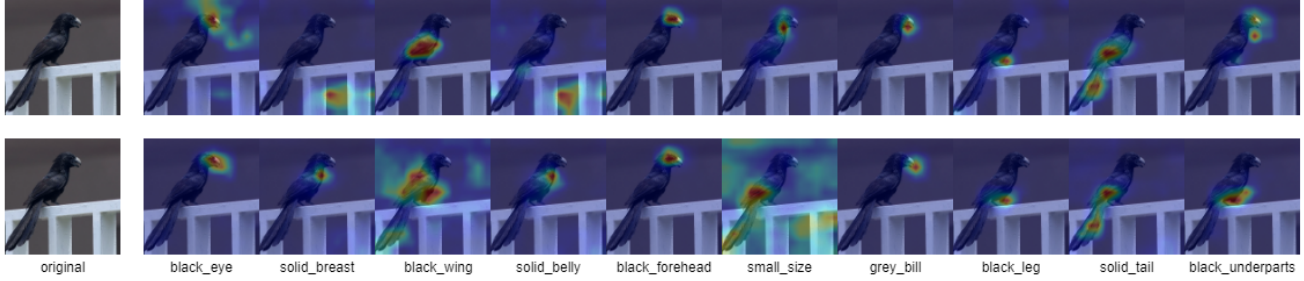


Figure 5. Visualization of the attention heat map. The first row represents the heat map of MSDN and the second row denotes our method (better viewed in color).

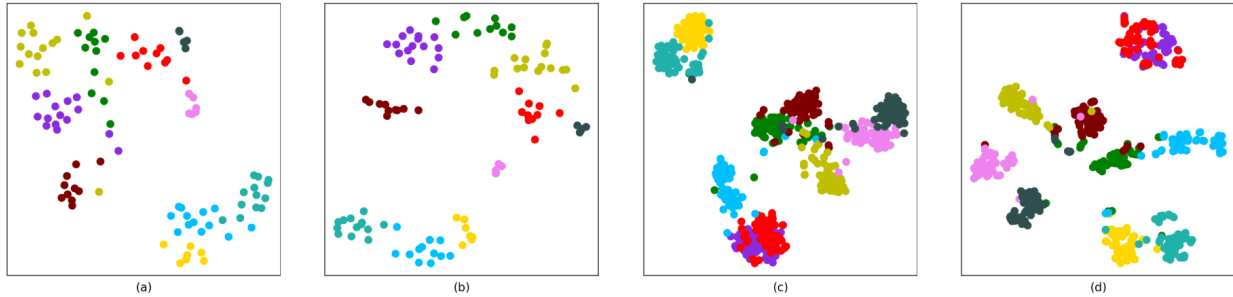


Figure 6. The t-SNE visualization of our method and MSDN. (a-b): seen class features; (c-d): unseen class features. (a, c): MSDN, (b, d): Our method (better viewed in color).

mitigating forgetting and overfitting. The experimental results are shown in Fig. 3. In the figure, the horizontal axis represents the training time, i.e., the training epoch. Fig. 3 (a) and (b) represent the results with the learning rate as $5e-6$, Fig. 3 (c) represents the results with the learning rate as $5e-5$, and Fig. 3 (d) represents the results with the learning rate as $1e-5$. From the figures, it can be seen that our method is relatively more stable, especially the results in Fig. 3 (a) and Fig. 3 (b), which show that our method can effectively suppress the forgetting problem of the model. In Fig. 3 (c) and Fig. 3 (d), there are fluctuations caused by the excessive learning rate, but our method can adjust quickly and obtain higher performance than fine-tuning. It indicates that our AGL module effectively captures the attribute-related features and boosts the performance.

4.5. Visualization of Attribute-Region Attention

In order to investigate the features that our scheme keeps and learns during the learning process, we perform a visualization analysis. As shown in Fig. 5, the first row represents the baseline method, and the second row is our method. It can be seen that MSDN endeavors to learn as much as it can about the correspondence between attributes and visual features, but it still constructs some wrong relational pairs. Our method preserves the features that correspond cor-

rectly, e.g., *black_wing*, *black_forehead*, *grey_bill*. Meanwhile, features that are not originally learned are successfully enhanced or captured by our scheme, e.g., *black_eye*, *solid_breast*, *solid_belly*, *black_underparts*. It illustrates that our method effectively maintains the original valuable knowledge and guides the model to mine more attribute-related features.

4.6. t-SNE Analysis to Features

We utilize the t-SNE map on CUB to study the kept and learned features. The experimental results are shown in Fig. 6, where 10 classes are randomly selected. From the image, we can observe that our method is effective for both seen and unseen classes. Specifically, the features extracted by our method possess more obvious differentiation, e.g., *green*, *purple*, *yellowgreen* in Fig. 6 (b) and *yellow*, *cyan*, *pink* in Fig. 6 (d). It demonstrates that the proposed AGL module effectively captures the connection between features and attributes, and thus learns the attribute-related knowledge and transfers it to the unseen domain.

5. Conclusion

In this paper, we analyze that existing ZSL/GZSL methods are limited by the incompleteness of the extracted features. Such incompleteness stems from the problem of domain

bias between the pre-trained model and the downstream tasks. Fine-tuning serves as a simple approach to address this problem, while can introduce catastrophic forgetting and seen class biased overfitting. To address these issues, we present a novel Attribute-Aware Representation Rectification framework, dubbed (AR)², to refine the learned features while, at the same time, maintaining the original valuable features. Our approach consists of two main modules, i.e., Unseen-Aware Distillation (UAD) and Attribute-Guided Learning (AGL), which dominate the work of keeping old knowledge and learning effective new knowledge, respectively. Through extensive experimental analysis, we show that our method can effectively improve the model's recognition performance in ZSL/GZSL tasks.

References

- [1] Soravit Changpinyo, Wei-Lun Chao, Boqing Gong, and Fei Sha. Synthesized classifiers for zero-shot learning. In *Proceedings of the IEEE Conference on Computer Vision and Pattern Recognition*, pages 5327–5336, 2016. 3
- [2] Wei-Lun Chao, Soravit Changpinyo, Boqing Gong, and Fei Sha. An empirical study and analysis of generalized zero-shot learning for object recognition in the wild. In *Computer Vision—ECCV 2016: 14th European Conference, Amsterdam, The Netherlands, October 11–14, 2016, Proceedings, Part II 14*, pages 52–68. Springer, 2016. 2
- [3] Shiming Chen, Wenjie Wang, Beihao Xia, Qinmu Peng, Xinge You, Feng Zheng, and Ling Shao. Free: Feature refinement for generalized zero-shot learning. In *Proceedings of the IEEE/CVF International Conference on Computer Vision*, pages 122–131, 2021. 2, 3, 6
- [4] Shiming Chen, Guosen Xie, Yang Liu, Qinmu Peng, Baigui Sun, Hao Li, Xinge You, and Ling Shao. Hsva: Hierarchical semantic-visual adaptation for zero-shot learning. *Advances in Neural Information Processing Systems*, 34:16622–16634, 2021. 6
- [5] Shiming Chen, Ziming Hong, Yang Liu, Guo-Sen Xie, Baigui Sun, Hao Li, Qinmu Peng, Ke Lu, and Xinge You. Transzero: Attribute-guided transformer for zero-shot learning. In *Proceedings of the AAAI Conference on Artificial Intelligence*, pages 330–338, 2022. 2, 3
- [6] Shiming Chen, Ziming Hong, Guo-Sen Xie, Wenhan Yang, Qinmu Peng, Kai Wang, Jian Zhao, and Xinge You. Msdn: Mutually semantic distillation network for zero-shot learning. In *Proceedings of the IEEE/CVF Conference on Computer Vision and Pattern Recognition*, pages 7612–7621, 2022. 2, 3, 6
- [7] Zhi Chen, Yadan Luo, Ruihong Qiu, Sen Wang, Zi Huang, Jingjing Li, and Zheng Zhang. Semantics disentangling for generalized zero-shot learning. In *Proceedings of the IEEE/CVF International Conference on Computer Vision*, pages 8712–8720, 2021. 3, 6
- [8] Zhi Chen, Pengfei Zhang, Jingjing Li, Sen Wang, and Zi Huang. Zero-shot learning by harnessing adversarial samples. In *Proceedings of the 31st ACM International Conference on Multimedia*, pages 4138–4146, 2023. 6
- [9] Matthias De Lange, Rahaf Aljundi, Marc Masana, Sarah Parisot, Xu Jia, Aleš Leonardis, Gregory Slabaugh, and Tinne Tuytelaars. A continual learning survey: Defying forgetting in classification tasks. *IEEE Transactions on Pattern Analysis and Machine Intelligence*, 44(7):3366–3385, 2021. 2
- [10] Jia Deng, Wei Dong, Richard Socher, Li-Jia Li, Kai Li, and Li Fei-Fei. Imagenet: A large-scale hierarchical image database. In *2009 IEEE Conference on Computer Vision and Pattern Recognition*, pages 248–255. Ieee, 2009. 2, 3, 6
- [11] Rafael Felix, Ian Reid, Gustavo Carneiro, et al. Multi-modal cycle-consistent generalized zero-shot learning. In *Proceedings of the European Conference on Computer Vision*, pages 21–37, 2018. 2, 3
- [12] Robert Geirhos, Jörn-Henrik Jacobsen, Claudio Michaelis, Richard Zemel, Wieland Brendel, Matthias Bethge, and Felix A Wichmann. Shortcut learning in deep neural networks. *Nature Machine Intelligence*, 2(11):665–673, 2020. 2, 5
- [13] Jingcai Guo, Song Guo, Qihua Zhou, Ziming Liu, Xiaocheng Lu, and Fushuo Huo. Graph knows unknowns: Reformulate zero-shot learning as sample-level graph recognition. 37(6): 7775–7783, 2023. 2, 3
- [14] Zongyan Han, Zhenyong Fu, Shuo Chen, and Jian Yang. Contrastive embedding for generalized zero-shot learning. In *Proceedings of the IEEE/CVF Conference on Computer Vision and Pattern Recognition*, pages 2371–2381, 2021. 3, 6
- [15] Kaiming He, Xiangyu Zhang, Shaoqing Ren, and Jian Sun. Deep residual learning for image recognition. In *Proceedings of the IEEE Conference on Computer Vision and Pattern Recognition*, pages 770–778, 2016. 6
- [16] Dan Hendrycks, Kimin Lee, and Mantas Mazeika. Using pre-training can improve model robustness and uncertainty. In *International Conference on Machine Learning*, pages 2712–2721. PMLR, 2019. 2, 3
- [17] Dat Huynh and Ehsan Elhamifar. Fine-grained generalized zero-shot learning via dense attribute-based attention. In *Proceedings of the IEEE/CVF Conference on Computer Vision and Pattern Recognition*, pages 4483–4493, 2020. 2, 3, 6
- [18] Huajie Jiang, Ruiping Wang, Shiguang Shan, and Xilin Chen. Transferable contrastive network for generalized zero-shot learning. In *Proceedings of the IEEE/CVF International Conference on Computer Vision*, pages 9765–9774, 2019. 3
- [19] Rohit Keshari, Richa Singh, and Mayank Vatsa. Generalized zero-shot learning via over-complete distribution. In *Proceedings of the IEEE/CVF Conference on Computer Vision and Pattern Recognition*, pages 13300–13308, 2020. 2, 3
- [20] Elyor Kodirov, Tao Xiang, and Shaogang Gong. Semantic autoencoder for zero-shot learning. In *Proceedings of the IEEE Conference on Computer Vision and Pattern Recognition*, pages 3174–3183, 2017. 3
- [21] Xia Kong, Zuodong Gao, Xiaofan Li, Ming Hong, Jun Liu, Chengjie Wang, Yuan Xie, and Yanyun Qu. En-compactness: Self-distillation embedding & contrastive generation for generalized zero-shot learning. In *Proceedings of the IEEE/CVF Conference on Computer Vision and Pattern Recognition*, pages 9306–9315, 2022. 3

- [22] Christoph H Lampert, Hannes Nickisch, and Stefan Harmeling. Learning to detect unseen object classes by between-class attribute transfer. In *2009 IEEE Conference on Computer Vision and Pattern Recognition*, pages 951–958. IEEE, 2009. [2](#)
- [23] Hao Li, Pratik Chaudhari, Hao Yang, Michael Lam, Avinash Ravichandran, Rahul Bhotika, and Stefano Soatto. Rethinking the hyperparameters for fine-tuning. In *International Conference on Learning Representations*, 2019. [2, 3](#)
- [24] Jingjing Li, Mengmeng Jing, Ke Lu, Zhengming Ding, Lei Zhu, and Zi Huang. Leveraging the invariant side of generative zero-shot learning. In *Proceedings of the IEEE/CVF Conference on Computer Vision and Pattern Recognition*, pages 7402–7411, 2019. [2, 3](#)
- [25] Xiangyu Li, Zhe Xu, Kun Wei, and Cheng Deng. Generalized zero-shot learning via disentangled representation. In *Proceedings of the AAAI Conference on Artificial Intelligence*, pages 1966–1974, 2021. [3](#)
- [26] Xiaofan Li, Yachao Zhang, Shiran Bian, Yanyun Qu, Yuan Xie, Zhongchao Shi, and Jianping Fan. Vs-boost: Boosting visual-semantic association for generalized zero-shot learning. In *International Joint Conference on Artificial Intelligence*, 2023. [3, 6](#)
- [27] Lu Liu, Tianyi Zhou, Guodong Long, Jing Jiang, and Chengqi Zhang. Attribute propagation network for graph zero-shot learning. In *Proceedings of the AAAI Conference on Artificial Intelligence*, pages 4868–4875, 2020. [3](#)
- [28] Shichen Liu, Mingsheng Long, Jianmin Wang, and Michael I Jordan. Generalized zero-shot learning with deep calibration network. *Advances in Neural Information Processing Systems*, 31, 2018. [3, 6](#)
- [29] Yang Liu, Jishun Guo, Deng Cai, and Xiaofei He. Attribute attention for semantic disambiguation in zero-shot learning. In *Proceedings of the IEEE/CVF International Conference on Computer Vision*, pages 6698–6707, 2019. [6](#)
- [30] Sanath Narayan, Akshita Gupta, Fahad Shahbaz Khan, Cees GM Snoek, and Ling Shao. Latent embedding feedback and discriminative features for zero-shot classification. In *Computer Vision—ECCV 2020: 16th European Conference, Glasgow, UK, August 23–28, 2020, Proceedings, Part XXII 16*, pages 479–495. Springer, 2020. [6](#)
- [31] Genevieve Patterson and James Hays. Sun attribute database: Discovering, annotating, and recognizing scene attributes. In *2012 IEEE Conference on Computer Vision and Pattern Recognition*, pages 2751–2758. IEEE, 2012. [5](#)
- [32] Bernardino Romera-Paredes and Philip Torr. An embarrassingly simple approach to zero-shot learning. In *International Conference on Machine Learning*, pages 2152–2161. PMLR, 2015. [3](#)
- [33] Edgar Schonfeld, Sayna Ebrahimi, Samarth Sinha, Trevor Darrell, and Zeynep Akata. Generalized zero-and few-shot learning via aligned variational autoencoders. In *Proceedings of the IEEE/CVF Conference on Computer Vision and Pattern Recognition*, pages 8247–8255, 2019. [2, 3, 6](#)
- [34] Ramprasaath R Selvaraju, Michael Cogswell, Abhishek Das, Ramakrishna Vedantam, Devi Parikh, and Dhruv Batra. Grad-cam: Visual explanations from deep networks via gradient-based localization. In *Proceedings of the IEEE International Conference on Computer Vision*, pages 618–626, 2017. [2, 4](#)
- [35] Vinay Kumar Verma, Gundeep Arora, Ashish Mishra, and Piyush Rai. Generalized zero-shot learning via synthesized examples. In *Proceedings of the IEEE Conference on Computer Vision and Pattern Recognition*, pages 4281–4289, 2018. [2, 3](#)
- [36] Maunil R Vyas, Hemanth Venkateswara, and Sethuraman Panchanathan. Leveraging seen and unseen semantic relationships for generative zero-shot learning. In *Computer Vision—ECCV 2020: 16th European Conference, Glasgow, UK, August 23–28, 2020, Proceedings, Part XXX 16*, pages 70–86. Springer, 2020. [2, 3](#)
- [37] Catherine Wah, Steve Branson, Peter Welinder, Pietro Perona, and Serge Belongie. The caltech-ucsd birds-200-2011 dataset. 2011. [3, 5](#)
- [38] Chaoqun Wang, Shaobo Min, Xuejin Chen, Xiaoyan Sun, and Houqiang Li. Dual progressive prototype network for generalized zero-shot learning. *Advances in Neural Information Processing Systems*, 34:2936–2948, 2021. [3](#)
- [39] Yongqin Xian, Bernt Schiele, and Zeynep Akata. Zero-shot learning—the good, the bad and the ugly. In *Proceedings of the IEEE Conference on Computer Vision and Pattern Recognition*, pages 4582–4591, 2017. [5](#)
- [40] Yongqin Xian, Tobias Lorenz, Bernt Schiele, and Zeynep Akata. Feature generating networks for zero-shot learning. In *Proceedings of the IEEE Conference on Computer Vision and Pattern Recognition*, pages 5542–5551, 2018. [2, 3, 6](#)
- [41] Yongqin Xian, Saurabh Sharma, Bernt Schiele, and Zeynep Akata. f-vaegan-d2: A feature generating framework for any-shot learning. In *Proceedings of the IEEE/CVF Conference on Computer Vision and Pattern Recognition*, pages 10275–10284, 2019. [3, 6](#)
- [42] Guo-Sen Xie, Li Liu, Xiaobo Jin, Fan Zhu, Zheng Zhang, Jie Qin, Yazhou Yao, and Ling Shao. Attentive region embedding network for zero-shot learning. In *Proceedings of the IEEE/CVF Conference on Computer Vision and Pattern Recognition*, pages 9384–9393, 2019. [2, 3, 6](#)
- [43] Guo-Sen Xie, Li Liu, Fan Zhu, Fang Zhao, Zheng Zhang, Yazhou Yao, Jie Qin, and Ling Shao. Region graph embedding network for zero-shot learning. In *Computer Vision—ECCV 2020: 16th European Conference, Glasgow, UK, August 23–28, 2020, Proceedings, Part IV 16*, pages 562–580. Springer, 2020. [2, 3](#)
- [44] Guo-Sen Xie, Xu-Yao Zhang, Tian-Zhu Xiang, Fang Zhao, Zheng Zhang, Ling Shao, and Xuelong Li. Leveraging balanced semantic embedding for generative zero-shot learning. *IEEE Transactions on Neural Networks and Learning Systems*, 2022. [2, 3](#)
- [45] Wenjia Xu, Yongqin Xian, Jiuniu Wang, Bernt Schiele, and Zeynep Akata. Attribute prototype network for zero-shot learning. *Advances in Neural Information Processing Systems*, 33:21969–21980, 2020. [3, 6](#)
- [46] Wenjia Xu, Yongqin Xian, Jiuniu Wang, Bernt Schiele, and Zeynep Akata. Vgse: Visually-grounded semantic embeddings for zero-shot learning. In *Proceedings of the*

IEEE/CVF Conference on Computer Vision and Pattern Recognition, pages 9316–9325, 2022. 2, 3

- [47] Yunlong Yu, Zhong Ji, Jungong Han, and Zhongfei Zhang. Episode-based prototype generating network for zero-shot learning. In *Proceedings of the IEEE/CVF Conference on Computer Vision and Pattern Recognition*, pages 14035–14044, 2020. 2, 3, 6
- [48] Li Zhang, Tao Xiang, and Shaogang Gong. Learning a deep embedding model for zero-shot learning. In *Proceedings of the IEEE Conference on Computer Vision and Pattern Recognition*, pages 2021–2030, 2017. 3
- [49] Yizhe Zhu, Jianwen Xie, Zhiqiang Tang, Xi Peng, and Ahmed Elgammal. Semantic-guided multi-attention localization for zero-shot learning. *Advances in Neural Information Processing Systems*, 32, 2019. 6